

An Ultraviolet to Mid-Infrared Study of the Physical and Wind Properties of HD 164270 (WC9) and Comparison to BD+30 3639 ([WC9])

Paul A. Crowther

Department of Physics and Astronomy, University of Sheffield, Hicks Building, Hounsfield Rd, Sheffield, S3 7RH, UK

Paul.Crowther@sheffield.ac.uk

P. W. Morris

NASA Herschel Science Center, Caltech M/S 100-22, 1200 E. California Blvd, Pasadena, CA 91125

J. D. Smith

Steward Observatory, University of Arizona, Tucson, AZ 85721

ABSTRACT

We present new *Spitzer* IRS observations of HD 164270 (WC9, WR103). A quantitative analysis of the UV, optical, near- and mid-IR spectrum of HD 164270 is presented, allowing for line blanketing and wind clumping, revealing $T_* \sim 48\text{kK}$, $\log L/L_\odot \sim 4.9$, $\dot{M} \sim 10^{-5} M_\odot \text{ yr}^{-1}$ for a volume filling factor of $f \sim 0.1$. Our models predict that He is partially recombined in the outer stellar wind, such that recent radio-derived mass-loss rates of WC9 stars have been underestimated. We obtain C/He ~ 0.2 and O/He ~ 0.01 by number from optical diagnostics. Mid-IR fine structure lines of [Ne II] 12.8 μm and [S III] 18.7 μm are observed, with [Ne III] 15.5 μm and [S IV] 10.5 μm absent. From these we obtain Ne/He $\sim \text{Ne}^+/\text{He} = 2.2 \times 10^{-3}$ by number, 7 times higher than the Solar value (as recently derived by Asplund et al.), and S/He $\sim \text{S}^{2+}/\text{He} = 5.1 \times 10^{-5}$ by number. From a comparison with similar results for other WC subtypes we conclude that WC9 stars are as chemically advanced as earlier subtypes. We consider why late WC stars are exclusively observed in high metallicity environments. In addition, we compare the UV/optical/mid-IR spectroscopic morphology of HD 164270 with the Planetary Nebula central star BD+30 3639 ([WC9]). Their UV and optical signatures are remarkably similar, such that our quantitative comparisons confirm similarities in stellar temperature, wind densities and chemistry first proposed by Smith & Aller, in spite of completely different evolutionary histories,

with HD 164270 presently a factor of ten more massive than BD+30 3639. At mid-IR wavelengths, the dust from the dense young, nebula of BD+30 3639 completely dominates its appearance, in contrast with HD 164270.

Subject headings: stars: individual: HD 164270, BD+30 3639 – stars: Wolf-Rayet – infrared: stars – planetary nebulae: general

1. Introduction

It has long been known that low ionization, carbon sequence Wolf-Rayet stars (WC9 stars) are exclusively found within the inner, metal-rich disk of our Milky Way (van der Hucht 2001; Hopewell et al. 2005). No WC9 stars are known elsewhere in the Local Group of galaxies, despite numerous surveys (Heydari-Malayeri et al. 1990, Moffat 1991). Indeed, WC9 populations have only recently been identified elsewhere within the metal-rich spiral M 83 by Hadfield et al. (2005).

The link between late WC subtypes and metal-rich environments led Smith & Maeder (1991) to suggest that strong stellar winds at high metallicity reveal He-burning processed material at an earlier phase than at lower metallicity, which they attributed spectroscopically to late WC stars, i.e. a decreasing C/He abundance ratio at later WC subtypes. This has persisted in the literature through to the present time (e.g. Hirschi et al. 2005). In contrast, stellar atmosphere models of WC4–8 stars have concluded that there is no such trend with subtype (Koesterke & Hamann 1995). Alternatively, neglecting optical depth effects, recombination line theory may be applied to hydrogenic transitions of C IV in early WC stars (e.g. Smith & Hummer 1998). Since C II-III transitions dominate the optical appearance of late WC stars, recombination line studies of late WC stars are extremely challenging.

The advent of sensitive mid-IR spectrometers aboard *Infrared Space Observatory* and *Spitzer* allows alternative indicators of evolutionary status, via fine-structure lines from elements sensitive to advanced nucleosynthesis reactions, such as neon. Theoretically, at the start of He-burning one expects the rapid conversion of ^{14}N to ^{22}Ne , increasing the abundance of this isotope by a factor of ~ 100 . Together with the cosmically more abundant ^{20}Ne isotope, one would expect a factor of ~ 15 increase in the neon abundance. Following techniques pioneered by Barlow et al. (1988), Ne/He in WC stars may be determined from measuring fluxes of the [Ne II] $12.8\mu\text{m}$ and [Ne III] $15.5\mu\text{m}$ lines, the latter solely observed from space-based missions. Mid-IR studies with *ISO* have revealed high Ne abundances in WC6–8 stars (Willis et al. 1997; Dessart et al. 2000). The majority of late-type WC stars

are known to form carbon-rich dust, either persistent or episodically such that many are dust-dominated at mid-IR wavelengths (Williams et al. 1987). Due to poor sensitivity of the mid-IR *SWS* spectrometer, only dust dominated WC9 stars were observed with *ISO*, completely veiling the stellar wind signature in the mid-IR. To date, AS320 (WR121) is the only WC9 star for which a neon abundance has been obtained, albeit based solely on [Ne II] $12.8\mu\text{m}$ (Smith & Houck 2005).

In the current study, *Spitzer* IRS spectroscopy of HD 164270 (WR103, WC9) is presented. HD 164270 does possess a dust shell (van der Hucht 2001), although this is sufficiently faint that stellar wind lines are observed in the mid-IR, including the crucial fine-structure lines of Ne and S. In order to derive neon and sulfur abundances, we perform the first quantitative study of a WC9 star allowing for non-LTE radiative transfer in an extended, clumped, expanding atmosphere allowing for metal line blanketing (Hillier & Miller 1998).

Finally, we carry out the first modern comparison between the chemical and wind properties of HD 164270 and BD+30 3639 ([WC9], alias HD 184738, Campbell 1893). The latter represents one of a small group of central stars of Planetary Nebulae (CSPNe) which share the spectroscopic appearance of WC stars. Smith & Aller (1971) carried out an optical qualitative spectroscopic comparison of these two stars and concluded that they were virtually identical, except for narrower wind lines and strong nebular lines in the CSPN. BD+30 3639 is located in a young (800 yr) compact nebula ($4''$ in diameter, Li et al. 2002) whilst HD 164270, as with most Population I WC stars, is not associated with an optically visible nebula. As with some dusty WC stars, PNe with late-[WC] type central stars are very bright at mid-IR wavelengths due to hot dust within their compact, dense nebulae, so were readily observed with *ISO/SWS* (e.g. Waters et al 1998). In general, the material around massive Wolf-Rayet stars known to have circumstellar nebulae may contain dust condensed in one or more slow-moving outflows from previous mass-loss episodes, or by interactions with the ISM.

Although both WC and [WC] stars involve hydrogen deficient stars at a late stage of evolution, their evolutionary paths followed are remarkably different. WC stars represent the final phase of initially very massive stars ($\geq 25M_{\odot}$ at Solar metallicity) undergoing advanced stages of nucleosynthesis prior to core-collapse as a Supernova. WC stars, with ages of $\sim 5\text{Myr}$, thus represent the bare cores of massive stars due to extensive stellar winds and exhibit the products of core He-burning (Meynet & Maeder 2003). In contrast, it is thought that [WC] stars result from low initial mass ($\sim 2M_{\odot}$) progenitors following the Asymptotic Giant Branch (AGB) phase. The hydrogen-rich stellar envelope of AGB stars may be removed in a late thermal pulse following shell H and He burning (Iben et al. 1983; Herwig et al. 1999), resulting in H-deficient post-AGB stars, CSPNe and ultimately white

dwarfs.

2. Observations

Our study uses far-UV to mid-IR spectroscopy of HD 164270 and BD+30 3639, of which *Spitzer* IRS mid-IR spectroscopy of HD 164270 is newly presented here.

2.1. Mid-IR/near-IR spectroscopy

HD 164270 was observed on 2004 March 4 (AOR key 6012160), with the *Spitzer*-IRS (Houck et al. 2004) as part of the Guaranteed Time Program WRDUST, using the long-slit Short-Low (SL) module at a spectral resolution $R \equiv \lambda/\Delta\lambda \simeq 75 - 125$, and the Short-High (SH) and Long-High (LH) echelle modules each at $R \simeq 1000$. These cover the wavelength ranges of $5.3 - 14.5 \mu\text{m}$ (SL), $10 - 19.5 \mu\text{m}$ (SH), and $19 - 37.5 \mu\text{m}$ (LH). Once the telescope’s pointing was re-initialized to an accuracy of $\leq 1''.0$ (1σ radial) using high accuracy peakup on a nearby offset star with the $16 \mu\text{m}$ camera in the IRS, the spectral observations were carried out in Staring Mode, which points the telescope so that the star is observed at two separate positions along the length of each slit, in principle allowing one to make background (zodiacal light and cirrus) emission corrections and mitigating the residual effects of incident cosmic rays and solar particles. The spectra were obtained using total integration times of 84, 480, and 360 seconds in the SL, SH, and LH modules, respectively. Background and pixel corrections in the noddled observations works in practice only for the SL observations, but cannot be achieved with the relatively short SH and LH slits without dedicated off-source observations, which we did not acquire. Background corrections to the SH and LH portions were therefore applied using the background model available from the *Spitzer* Science Center¹, normalized to the background levels observed with the SL portion at $10 \mu\text{m}$. Corrections to outlier pixels are discussed below.

Raw data cubes were processed on a pixel basis in the SSC pipeline (S10.5), which re-formats the pixel data and housekeeping information, removes dark currents and multiplexer drift, applies corrections for inter-pixel photocurrent coupling and amplifier non-linearities, fits the integration ramps and reduces the data cubes to 2-dimensional signal planes in units of electrons/sec/pixel. At this point we removed the background levels in the SL data, defined approximately $1'$ on either side of the star in the off-source subslits. The result-

¹<http://ssc.spitzer.caltech.edu/documents/background/>

ing illumination profile at each wavelength was found to be consistent with that of a point source (no extended emission was detected), and subsequent photometric point-source calibrations were applied during spectral extraction. Prior to extraction of the SH and LH data, however, we made systematic outlier pixel corrections using preceding dark current measurements obtained on the “blank” sky at the North Ecliptic Pole. The default superdarks subtracted in this version of the pipeline are combined from measurements over several observing campaigns, but the offline use of nearest-in-time dark currents provides a more accurate, contemporaneous match to individual pixels with dark currents varying over several hours to a day. Remaining dead pixels in the illuminated regions of the arrays (totaling less than 5%) were corrected by a spline interpolation scheme. Spectra from each individual integration were then extracted using offline SSC software, applying wavelength calibrations accurate to $\sim 1/5$ resolution element for well-pointed observations (± 0.02 and $0.002 \mu\text{m}$ in SL and SH spectra at $10\mu\text{m}$, and $\pm 0.005 \mu\text{m}$ in LH at $25 \mu\text{m}$). Individual spectra were then examined and combined. Photometric uncertainties are estimated to be 5% for SL, 5 – 15% for SH, and 15 – 20% for LH (increasing with wavelength due to the approximations of the background levels). However, we find excellent agreement between our flux-calibrated IRS spectra and ground-based L, M and N-band photometry, discussed below.

The IRS spectrum of HD 164270 is described by a blue stellar continuum, with a number of spectral features superimposed. We present selected regions of the IRS spectrum in Fig. 1, revealing a combination of spectral lines from He I and C II formed in the inner stellar wind, plus fine-structure lines from [Ne II] $12.8\mu\text{m}$ and [S III] $18.7\mu\text{m}$ formed in the outer stellar wind, with [Ne III] $15.5\mu\text{m}$ and [S IV] $10.5\mu\text{m}$ notably absent. We have measured the line fluxes from the fine-structure lines to be $F_\lambda([\text{Ne II}]) = 2.18 \pm 0.08 \times 10^{-12} \text{ erg/s/cm}^2$, and $F_\lambda([\text{S III}]) = 1.03 \pm 0.01 \times 10^{-13} \text{ erg/s/cm}^2$.

For BD+30 3639 we use the combined ISO SWS/LWS spectrum from Cohen et al. (2002), namely TDT35501531 (SWS01) and TDT35501412 (LWS01) observed in Nov 1996, to which the reader is referred for detailed information. The mid-IR continuum is reproduced by two temperature blackbodies (290 and 98K) plus crystalline and amorphous silicate features (Waters et al. 1998). No stellar spectral features are observed due to the dominant dust signature. [Ne II] $12.8\mu\text{m}$ and [S III] $18.7\mu\text{m}$ are also observed in BD+30 3639, although these are nebular in origin within this system. The neutral nebular mass amounts to $0.13M_\odot$ for a distance of 1.2 kpc as derived from the ISO/LWS [C II] $158\mu\text{m}$ line flux (Liu et al. 2001).

We have also used near-IR spectroscopy of HD 164270 obtained with the 3.8m UK Infrared Telescope (UKIRT) from August 1994. The cooled grating spectrograph CGS4, 300mm camera, 75l/mm grating and a 62×58 InSb array were used to observe three non-overlapping settings, covering $1.03\text{--}1.13\mu\text{m}$ ($\lambda/\Delta\lambda = 800$), $1.61\text{--}1.82\mu\text{m}$ ($\lambda/\Delta\lambda = 600$) and

2.01–2.21 μm ($\lambda/\Delta\lambda = 800$). Details of the data reduction are provided by Crowther & Smith (1996). Eenens & Williams (1994) derive a wind velocity of 1100 km/s using their higher spectral resolution He I 2.058 μm observations of HD 164270.

2.2. UV/optical spectroscopy

Flux calibrated optical spectroscopy of HD 164270 were obtained with the 3.9m Anglo Australian Telescope and RGO spectrograph in November 1992 with a 1024x1024 Tektronix CCD, 1200V grating and 250mm camera, providing complete coverage between $\lambda\lambda 3680$ –6000 in three overlapping settings at 1.7 \AA resolution. For BD+30 3639, flux calibrated spectroscopy was obtained at the 4.2m William Herschel Telescope, together with the dual-beam ISIS spectrograph in August 2002. ISIS was equipped with an EEV CCD and 300B grating (blue) and a Marconi CDD and 300R grating (red) plus the $\lambda 6100$ dichroic, providing complete spectral coverage between $\lambda\lambda 3400$ –8800 at 3.5 \AA resolution. A standard reduction was applied in both cases using calibration arc lamps and spectrophotometric standard stars (e.g. see Crowther et al. 1998 for further details). Modern optical spectroscopy supports the findings of Smith & Aller (1971), with selected (classification) spectral regions presented in Fig. 2.

UV high dispersion, large aperture spectroscopy of both targets was obtained from the *IUE* Newly Extracted Spectra (INES) archive, namely SWP8156 and LWP13972 for HD 164270, with SWP7594, 7642, 8591, 8863, 13333, 51870 and LWR6924, 7334 for HD 164270. Stellar wind velocities (v_{black}) have been measured for Si IV $\lambda 1394$, revealing 1140 ± 50 km/s for HD 164270 (Prinja et al. 1990) and 700 ± 50 km/s for BD+30 3639. These values are adopted for the remainder of this analysis.

Finally, we also used *Far-Ultraviolet Spectroscopic Explorer (FUSE)* spectroscopy of HD 164270 covering $\lambda\lambda 912$ –1190 \AA , namely *FUSE* dataset P1171001 with an exposure time of 5.1ks, as discussed in Willis et al. (2004). Our adopted wind velocity of HD 164270 is in reasonable agreement with the average velocity of 1036 km/s in Willis et al.

2.3. Distances and interstellar reddening

We adopt spectrophotometry of HD 164270 from Torres-Dodgen & Massey (1988), revealing a narrow-band (Smith 1968) visual magnitude of $v=8.86$ mag, whilst we adopt $M_v = -4.6 \pm 0.4$ mag for WC9 subtypes, based on estimated absolute magnitudes for three Galactic WC9 stars from van der Hucht (2001). High resolution spectroscopy of several WC9

stars reveals the characteristic signature of a luminous OB-type companion (Williams & van der Hucht 2000), but no evidence of a luminous companion to HD 164270 is known (Smith & Aller 1971). From our spectral fits we estimate $E(b - v)=0.49$ ($E(B - V)=0.58$) using $R=A_V/E(B - V)=3.0$ which indicates a distance of ~ 1.9 kpc to HD 164270.

For BD+30 3639, our WHT spectrophotometry indicates $v = 10.28$ mag. Li et al. (2002) have recently analysed WFPC2 images obtained 5 yr apart to measure the PN expansion rate and so derive a distance of 1.2 kpc which together with our estimate of $E(b - v)=0.32$ ($E(B - V) = 0.39$) indicates $M_v = -1.5$ mag.

2.4. Dust modeling

De-reddened spectrophotometric flux distributions from 0.1 to $100\mu\text{m}$ are presented in Fig. 3, together with ground-based photometry from 2MASS, Williams et al. (1987) and Jameson et al. (1974), and theoretical continua obtained from our analysis. These illustrate the UV/optical similarities, and mid-IR differences between HD 164270 and BD+30 3639. Dust contributes negligibly to the total energy budget of HD 164270, whilst the (re-radiated) dust in BD+30 3639 is comparable to the stellar flux. We adopt a standard Galactic extinction law ($R=3.1$) for the UV/optical/near-IR (Howarth 1983), supplemented with a mid-IR extinction curve provided by M. Cohen (see Fig.2 of Morris et al. 2000).

Since the primary goal of the current study is to investigate the physical and wind properties of WC9 stars, we use dust radiative transfer models from the recent literature. For HD 164270, we use a dust spectral energy distribution from TORUS (Harries, priv comm.) following the approach of Harries et al. (2004) for WR104. The TORUS model assumes a spherical shell composed of amorphous carbon with a uniform size of $0.1\mu\text{m}$ and a dust-to-gas ratio of 2×10^{-5} by mass. With respect to other very dusty WC9 stars (van der Hucht et al. 1996), the dust shell associated with HD 164270 is relatively weak, contributing at most 80% of the continuum flux at $3\mu\text{m}$.

For the dust associated with BD+30 3639 we use the MODUST model presented by Waters et al. (1998), who identified distinct (cooler) O-rich and (warmer) C-rich shells. The MODUST model is successful in reproducing the observed energy distribution longward of 10μ , where dust contributes greater than 99.9% of the continuum flux, but fails to reproduce the 1– $10\mu\text{m}$ excess. For both HD 164270 and BD+30 3639, dust emission contaminates the stellar flux distribution longward of $1.3\mu\text{m}$.

3. Quantitative analysis

3.1. Technique

For the present study we employ CMFGEN (Hillier & Miller 1998), which solves the transfer equation in the co-moving frame subject to statistical and radiative equilibrium, assuming an expanding, spherically-symmetric, homogeneous and static atmosphere, allowing for line blanketing and clumping. The stellar radius (R_*) is defined as the inner boundary of the model atmosphere and is located at Rosseland optical depth of ~ 20 with the stellar temperature (T_*) defined by the usual Stefan-Boltzmann relation.

Our approach follows previous studies (e.g. Crowther et al. 2002), such that diagnostic optical lines of C II $\lambda 4267$, C III $\lambda 5696$ and C IV $\lambda \lambda 5801-12$ plus the local continuum level allow a determination of the stellar temperature, mass-loss rate and luminosity. In contrast with earlier WC subtypes, a reliable treatment of low temperature de-electronic recombination C II lines is necessary in WC9 stars. These lines are not included in Opacity Project calculations, so improved SUPERSTRUCTURE calculations were carried out by P.J. Storey on our behalf.

Our final model atom contains He I-II, C II-IV, O II-IV, Ne II-IV, Si III-IV, S III-VI, Ar III-V, Ca II-VI and Fe III-VI. In total, 987 super levels, 3497 full levels and 40,952 non-LTE transitions are simultaneously considered. We assume hydrogen is absent, with variable C, O and Ne abundances, and Si-Fe initially fixed at Solar values (Grevesse & Sauval 1998). As for other WC subtypes, C/He abundances are ideally obtained from He II $\lambda 5411$ and C IV $\lambda 5471$. Since these lines are weak in WC9 stars, the accuracy with which C/He may be obtained in this way is reduced relative to earlier subtypes, but should be accurate to ± 0.1 by number. For oxygen, O II $\lambda 4415-4417$, O III $\lambda 3754-3759$, $\lambda 5592$ provide the cleanest oxygen diagnostics in the visual region, and should permit a determination of O/He to within a factor of two. Williams & van der Hucht (2000) revealed that WC9 stars span a range in O II $\lambda 4415-4417$ line strength, suggesting a factor of ≥ 2 spread in oxygen abundance.

We adopt a standard form of the velocity law, $v(r) = v_\infty(1 - R_*/r)^\beta$, where $\beta=1$. The mass-loss rate is actually derived as the ratio \dot{M}/\sqrt{f} , where f is the volume filling factor that can be constrained by fits to the electron scattering wings of the helium line profiles (following Hillier 1991) resulting in $f \sim 0.1$. From the observed strength of electron scattering wings we can definitely exclude homogeneous mass-loss in both HD 164270 and BD+30 3639.

3.2. Physical and Wind properties

We compare our synthetic model of HD 164270 to de-reddened UV (*IUE*) and optical (AAT) spectroscopic observations in Fig. 4. The agreement between the spectral features and continuum is generally excellent. The majority of synthetic near-UV and optical (primarily He, C, O) lines match observations to within $\sim 30\%$. The only exception is C III $\lambda 4647\text{--}50$ which is too weak. This can be resolved with a 5% higher temperature, at the expense of other fits to optical lines. In the far-UV, numerous Fe features dominate the spectral appearance, together with C and Si resonance lines. The synthetic Fe spectrum is generally too strong in emission, as are Si III $\lambda 1295\text{--}1312$ and the blue component of Si IV $\lambda 1393\text{--}1402$, whilst C III $\lambda 2297$ is 30% too weak. C IV $\lambda 1548\text{--}51$ is too weak in emission at a stellar temperature of 48kK. As with C III $\lambda 4647\text{--}51$, this can be reproduced at a slightly higher temperature, albeit with poorer agreement in the iron forest around $\lambda 1450$.

We compare the de-reddened *FUSE* far-UV spectrum of HD 164270 to the synthetic spectrum in Fig. 5. Agreement is reasonable longward of $\lambda 1120$, where few molecular H₂ lines are absent, including the Si IV $\lambda 1122\text{--}28$ doublet, whilst Lyman and Werner molecular bands dominate the spectrum at shorter wavelengths, as demonstrated by the apparent absence of the C II $\lambda 1037$ in the *FUSE* dataset (see also Willis et al. 2004).

For completeness, we compare UV (*IUE*) and optical (WHT) spectrophotometry of BD+30 3639 to our synthetic model in Fig. 6. Comments are as for HD 164270, except for the strong nebular emission superimposed upon the stellar spectrum. The stellar parameters derived for each star are presented in Table 1. The derived stellar temperature of BD+30 3639 is higher than HD 164270 due to its smaller physical size, whilst their wind efficiencies, $\eta = \dot{M}v_\infty/(L/c)$ are effectively identical, despite stellar masses a factor of ten different. Mass estimates originate from the H-free mass-luminosity relation of Schaerer & Maeder (1992) for HD 164270, and Herwig et al. (1999) for BD+30 3639.

Recent theoretical (Herwig et al. 2003) and observational (Reiff et al. 2005) evidence suggests that H-deficient PG1159 stars (for which [WC] subtypes are likely precursors) are severely Fe-depleted. Thus far we have adopted Solar (Grevesse & Sauval 1998) heavy metal abundances. Consequently, we additionally considered models in which the iron content is reduced by a factor of ten with respect to Solar. This reduced iron model compares rather more favorably to observation in the $\lambda 1400\text{--}1700$ region (Fe IV–V), whilst the Solar Fe model is in better agreement for $\lambda \geq 1800$ (also Fe IV). Recall, however that the synthetic far-UV spectrum for HD 164270 was also rather too strong with respect to observations, so a more robust result awaits improved spectroscopic fits across the entire far-UV. Fortunately, the question of Fe depletion in BD+30 3639 does not affect our main aim of the present study, since the optical spectroscopic appearance of the Solar and Fe-depleted models are virtually

identical.

3.3. Comparison with previous results

Our derived stellar temperature of $T_* \sim 48\text{kK}$ for HD 164270 is rather higher than the previous estimate of 30kK for WC9 stars, based on pure helium model atmospheres (Howarth & Schmutz 1992). This follows the general trend in which the inclusion of line blanketing leads to an increase in stellar temperatures for WR stars (Crowther 2003b). The present study represents the first detailed investigation of any WC9 star, it is in good agreement with the estimate of 45kK for WR104 by Crowther (1997) using a He, C and O non-LTE model.

Since late-WC stars are preferentially dust formers, we note that the ionizing flux distribution of HD 164270 is rather harder than those commonly adopted in chemical and radiative transfer studies of dust in such environments (e.g. Williams et al. 1987; Cherchneff et al. 2000). One notable exception is the 3D dust radiative transfer study of WR104 (Pinwheel nebula) by Harries et al. (2004) for which a similar stellar spectral energy distribution to the current study was adopted. The origins of dust around Population I late WC stars is still under debate, although recent studies suggest a binary system is required to provide H-rich material and the necessary shielding from the intense radiation for grain formation (Crowther 2003a). To date, there is no evidence for a luminous companion to HD 164270 (Smith & Aller 1971).

BD+30 3639 has been studied by Leuenhagen et al. (1996) using a non-LTE model atmosphere study, also allowing for He, C and O, such that blanketing and clumping were neglected. As with HD 164270, we obtain 55kK versus 47kK from Leuenhagen et al. (1996). However, blanketing tends to redistribute high energy photons to lower energy, leading to a softer ionizing flux distribution. In Table 1 we include the Lyman and HeI continuum ionizing fluxes for both stars. The relatively soft radiation explains why previous nebular techniques have obtained substantially lower estimates of the stellar temperature (e.g. 34kK : Siebenmorgen et al. 1994). In contrast to the amorphous carbon nature of dust associated with late WC stars (Williams et al. 1987), the PN associated with BD+30 3639 exhibits crystalline silicate dust, signaling a recent change from an oxygen- to carbon-dominated chemistry (Waters et al. 1998). De Marco et al. (2003) argue binarity could naturally explain the dual dust chemistry of PN and the H-depletion of the CSPN.

Finally, if we scale the Leuenhagen et al result for BD+30 3639 to our assumed distance of 1.2kpc , we obtain a revised luminosity of $\log L/L_\odot = 4.0$, versus 3.8 obtained here, and

a (homogeneous) mass-loss rate of $4 \times 10^{-6} M_{\odot} \text{ yr}^{-1}$ versus our estimate of $3 \times 10^{-6} M_{\odot} \text{ yr}^{-1}$.

3.4. Higher radio derived mass-loss rates for WC9 stars

Leitherer et al. (1997) obtained an upper limit to the 6cm radio flux for HD 164270 of $< 0.42 \text{ mJy}$, equating to a homogeneous mass-loss rate of $< 2.7 \times 10^{-5} M_{\odot} \text{ yr}^{-1}$ under the *assumption* of singly ionized He, C and O for the radio forming continuum, versus $\dot{M}/\sqrt{f} \sim 3 \times 10^{-5} M_{\odot} \text{ yr}^{-1}$ obtained here from an analysis of the UV, optical and near-IR spectrum. Since the radio estimate is recognized as providing the least model dependent mass-loss rates of Wolf-Rayet stars, does the present study contradict the radio results?

Fig. 7 presents the theoretical wind structure of our HD 164270 model, including the variation of electron temperature, electron density, velocity and stellar radius versus Rosse-land optical depth, together with the ionization balance of the principal elements, namely He, C, O, Fe. We also include Ne and S since we consider their ionization state in the outer winds in Sect. 3.5. The winds of WC9 stars are highly stratified, such that for example S^{6+} is the dominant ion of sulfur in the inner wind ($\sim 10^{14} \text{ cm}^{-3}$), whilst S^{2+} is the dominant ion in the outer wind ($\sim 10^7 \text{ cm}^{-3}$).

From the figure, our model atmosphere supports the dominant ionization stages of C^+ and O^+ in the outer wind, whilst He is partially recombined beyond several hundred R_{*} . Therefore, the claimed lower limit to the radio mass-loss rate by Leitherer et al. (1997) will increase. In fact, our model atmosphere predicts 2cm and 6cm radio fluxes of only 0.2mJy and 0.09mJy, respectively, for HD 164270. Similar arguments apply to the apparently low mass-loss rates of WC9 stars derived from radio observations by Cappa et al. (2004). As a consequence, their conclusions that WC9 stars possess weaker winds than earlier subtypes is not necessarily valid.

3.5. Elemental abundances

We admit a greater uncertainty in C/He for WC9 stars with respect to earlier WC stars due to the weakness of the diagnostic He II $\lambda 5411$ and C IV $\lambda 5471$ lines. We obtain $\text{C/He} \sim 0.2 \pm 0.1$ for HD 164270 and $\text{C/He} \sim 0.25 \pm 0.1$ for BD+30 3639, by number. O II lines at $\lambda 4415$ – 4417 , O III $\lambda 3754$ – 3759 , $\lambda 5592$ represent the primary abundance diagnostics, revealing $\text{O/He} \sim 0.01$ for HD 164270 and $\text{O/He} \sim 0.05$ for BD+30 3639, which ought to be reliable to a factor of two. No abundance studies have previously been reported for HD 164270, whilst Leuenhagen et al. (1996) derived $\text{C/He} = 0.37$ and $\text{O/He} = 0.03$, by number for BD+30 3639.

The fine-structure lines of [Ne II] 12.8 μm and [S III] λ 18.7 μm observed in HD 164270 (Fig. 1) permit the determination of ion fractions of Ne⁺ and S²⁺ in the outer wind of HD 164270. The critical densities for these fine-structure lines ($\sim 10^5 \text{ cm}^{-3}$) relate to the constant velocity regime at several thousand stellar radii in WC9 stars, comparable to the radio forming continuum. We determine abundances using numerical techniques introduced by Barlow et al. (1988), adapted to account for a clumped wind by Dessart et al. (2000) and Smith & Houck (2005). With regard to clumping, the volume filling factor within this region may be quite distinct from that estimated using optical recombination lines (Runacres & Owocki 2002).

The numerical expression for the ion number fraction, γ_i , in a clumped medium (with volume filling factor f) is (in cgs units)

$$\gamma_i = \frac{(4\pi\mu m_H v_\infty)^{1.5}}{\ln(10)f^{0.25}} \left(\frac{\sqrt{f}}{\dot{M}}\right)^{1.5} \frac{1}{F_u(T)} \frac{2D^2 I_{ul}}{\sqrt{\gamma_e} A_{ul} h\nu_{ul}} \quad (1)$$

where D is the stellar distance, I_{ul} is the line flux of the transition with energy $h\nu_{ul}$ between upper level u and lower level l , with transition probability A_{ul} . γ_e (=1.0) and T_e (=6000K) are the electron number density and temperature in the line-forming region, and the mean molecular weight is μ (=5.5) for HD 164270, with m_H the mass of the hydrogen atom. The integral part, $F_u(T)$, is

$$F_u(T) = \int_0^\infty \frac{f_u(N_e, T)}{\sqrt{N_e}} d\log(N_e). \quad (2)$$

where f_u is the fractional population of the upper level.

Following this technique, we derive $\gamma_{\text{Ne}^+} = 1.8 \times 10^{-3}$ and $\gamma_{\text{S}^{2+}} = 4.2 \times 10^{-5}$. Consequently, Ne⁺/He = 2.2 $\times 10^{-3}$ and S²⁺/He = 5.1 $\times 10^{-5}$ by number. Of course, one needs to account for potential contributions from unseen ionization stages. From Fig. 7, our model atmosphere predicts that Ne⁺ and S²⁺ are the dominant ions of neon and sulfur at the outer model radius of 1000 R_* , where $\log(n_e/\text{cm}^3) \sim 6.7$. A similar degree of ionization at $\log(n_e/\text{cm}^3) \sim 4.5\text{--}5.8$, where the [S III] and [Ne II] fine-structure lines form, is supported by the absence of the [S IV] 10.5 μm and [Ne III] 15.5 μm fine-structure lines, although we cannot exclude contributions from Ne⁰ and S⁺.

Consequently, we can set a lower limit to the Ne/He ratio with Ne⁺/He = 2.2 $\times 10^{-3}$. This implies a minimum mass fraction of neon of 0.7%, a factor of 7 times *higher* than the Solar value of Ne/H $\sim 7.2 \times 10^{-5}$ by number, as recently re-derived by Asplund et al. (2004) and Lodders (2003)². For sulphur, we can equally set a minimum abundance of sulfur with

²Note that the Bahcall et al. (2005) propose a higher Ne abundance of Ne/H=1.9 $\times 10^{-4}$ by number in or-

$S^{2+}/He = 5.1 \times 10^{-5}$. This indicates a minimum sulfur mass fraction of 0.024%, a factor of two times *lower* than the Solar mass fraction, with an unknown fraction singly ionized.

Smith & Houck (2005) have recently estimated the Ne abundance of AS320 (WR121, WC9d) based on ground-based [Ne II] $12.8\mu m$ spectroscopy. They estimated $Ne^+/He = 4.1 \times 10^{-3}$, based on the analytical approach of Barlow et al. (1998), a mass-loss rate that was 0.1 dex lower than a radio derived upper limit (though recall Sect 3.4), plus average C/He abundances for WC8–9 stars from the literature. The more accurate numerical technique applied above typically leads to a 10–20% reduction in ion abundance relative to the analytical approach. Since [Ne III] $15.5\mu m$ is unavailable from the ground, Smith & Houck (2005) inspected our HD 164270 *Spitzer* IRS dataset, which confirmed that Ne^+ instead of Ne^{2+} is the dominant ion in the outer wind of WC9 stars.

4. Discussion and Conclusions

We have presented the first quantitative, multi-wavelength spectroscopic study of a massive WC9 star, HD 164270. Overall, the non-LTE model is remarkably successful at reproducing the far-UV to mid-IR spectrum of HD 164270 such that we can be confident in the resulting physical and chemical properties.

With respect to earlier subtypes, WC9 stars genuinely possess lower stellar temperatures. However, we find a similar C/He for HD 164270 to earlier WC subtypes, based on identical abundance diagnostics, contrary to the decreasing C/He ratio for later WC subtypes proposed by Smith & Maeder (1991). This is emphasised in Fig. 8 which compares the carbon and neon abundances of all Galactic WC stars analysed by Dessart et al. (2000) to which we have added HD 164270. Chemically, WC9 stars therefore appear normal with respect to earlier WC subtypes. This conclusion is supported by Smith & Houck (2005) who estimated $Ne/He=4.1 \times 10^{-3}$ for another WC9 star, AS320, using ground-based spectroscopy, albeit with an uncertain, radio-derived mass-loss rate. Indeed, we shall suggest below that the presence of a WC dense wind intrinsically leads to a late-type WC star, so one might actually expect a substantial range of C/He within WC9 stars, as suggested by Williams et al. (2005).

In Fig. 8 we also include the predicted neon versus carbon enrichment during the WC stage for an initial $60M_{\odot}$ star at $Z=0.020$ initially rotating at 300 km/s from Meynet &

der to resolve the downward revised oxygen content of the Sun by Asplund et al. (2004) with helioseismology measurements.

Maeder (2003). HD 164270 supports the previous results from Dessart et al. (2000) that measured Ne enrichments fall a factor of 2–3 times lower than predictions. During the early WC phase it is ^{22}Ne enrichment by up to a factor of 200, rather than the initially more abundant ^{20}Ne which dominates the predicted enrichment. This increase is dictated by reaction rates and is unrelated to rotation (Meynet & Meynet 2003). Considering this poor agreement, a *Spitzer* guest investigator program is presently underway to study a larger sample of WC and WO stars to assess whether the relatively modest Ne enrichments obtained to date are typical.

Crowther et al. (2002) concluded that the defining characteristic distinguishing mid and early WC subtypes was primarily due to a higher wind density in the former, rather than significantly lower stellar temperature. One would be able to readily explain the observed preference of WC9 stars to inhabit high metallicity regions (e.g. Hopewell et al. 2005; Hadfield et al. 2005) if the wind strengths of WC stars increased with metallicity (Vink & de Koter 2005), i.e. high wind densities produce late subtypes, without the need for reduced stellar temperatures.

In contrast, radio mass-loss determinations of WC9 stars by Leitherer et al. (1997) and Cappa et al. (2004) suggest that they possess relatively low wind densities. However, helium is assumed to be singly ionized in radio mass-loss rate determinations, whilst Fig. 7 indicates that helium is partially recombined in the outer winds of WC9 stars. Consequently, previous radio mass-loss rate estimates for WC9 stars represent lower (rather than upper) limits.

In Fig. 9 we present the mass-loss rate versus luminosity relationship obtained for Galactic Wolf-Rayet stars by Nugis & Lamers (2000) for an assumed metal content of $\text{C}/\text{He}=0.25$ and $\text{C}/\text{O}=5$ by number, together with Galactic and LMC spectroscopic results from Crowther et al. (2002) and references therein, plus HD 164270. The generic relation of Nugis & Lamers is very successful at reproducing the mass-loss rates of Galactic WC5–7 stars. LMC WC4 stars possess low mass-loss rates for their high luminosities and γ Vel (WC8+O7.5 III) and HD 164270 (WC9) possess high mass-loss rates for their low luminosities. Despite our small sample, one might conclude that late WC stars result from high wind densities instead of low stellar temperatures. However, stellar temperatures of γ Vel (De Marco et al. 2000) and HD 164270 are the lowest of the entire sample, so the low ionization of WC8–9 stars appears to result from a combination of both high wind density and low stellar temperature.

Note that there is also an apparent trend for higher luminosities (masses) at earlier subtype in Fig. 9, although the reduced mass-loss rates prior to the Wolf-Rayet phase for the LMC stars relative to the Milky Way counterparts probably dominates this difference. Nevertheless, Galactic WC5–7 stars reveal higher present masses than WC8–9 stars (recall

all have well established distances with the exception of HD 164270).

The recent suggestion of severe Fe-depletion in the likely precursors of late [WC] stars (Herwig et al. 2003; Reiff et al. 2005) potentially impacts upon the ability of the star to exhibit a strong wind. Indeed, Gräfener & Hamann (2005) and Vink & de Koter (2005) both argue that winds of Wolf-Rayet stars are driven by radiation pressure with Fe-peak elements the principal components of the line driving. Consequently, a significant Fe depletion in BD+30 3639 might potentially reduce its wind density to significantly below that of HD 164270. Without the line driving from Fe-peak elements, [WC] subtypes may either be unlikely to occur, or possess very different wind properties from their Population I cousins. In contrast, we have demonstrated quantitatively that the winds of HD 164270 (WC9) and BD+30 3639 ([WC9]) are remarkably similar, supporting the earlier descriptive result from Smith & Aller (1971), despite very different evolutionary states, arguing against a severely depleted Fe-content in BD+30 3639.

Finally, we should emphasize that the physical and wind properties derived here for HD 164270 and BD+30 3639 are not based on self-consistent hydrodynamical models, i.e. mass-loss rates are imposed. Great progress towards such fully consistent models for Wolf-Rayet stars is now underway towards self-consistent wind models (notably Gräfener & Hamann 2005). In the meantime, from our comparison between WC and [WC] stars it appears that the combination of a hydrogen-deficient, metal-rich composition and intense radiation field are sufficient conditions for the development of a strong stellar wind, regardless of the evolutionary history (or present mass) of the star.

Thanks to John Hillier for providing CMFGEN and making modifications to incorporate new C II SUPERSTRUCTURE calculations by Pete Storey. Martin Cohen kindly provided the ISO spectrum of BD+30 3639. We also thank Tim Harries for calculating a dust model for HD 164270 with TORUS and Alex de Koter for providing the MODUST dust model for BD+30 3639. PAC acknowledges financial support from the Royal Society. This work is based in part on observations made with the WRDUST program (Principal Investigator J. Houck), using *Spitzer* Space Telescope, which is operated by the Jet Propulsion Laboratory, California Institute of Technology under NASA contract 1407. Support for this work was provided by NASA through an award issued by JPL/Caltech. This study also makes use of data products from the Two Micron All Sky Survey, which is a joint project of the University of Massachusetts and IPAC/CalTech, funded by NASA and the NSF, and from the NASA/IPAC Infrared Science Archive, which is operated by JPL/CalTech, under contract with NASA.

REFERENCES

- Asplund M., Grevesse N., Sauval A.J., Allende Prieto C., Kiselman, D., 2004, *A&A* 417, 751
- Bahcall J.N., Basu S., Serenelli A.M., 2005, *ApJ* submitted (astro-ph/0502563)
- Barlow M.J., Roche P.F., Aitken D.A., 1988, *MNRAS* 232, 821
- Campbell W.W., 1893, *PASP* 5, 204
- Cappa C., Goss W.M., van der Hucht K.A., 2004, *AJ* 127, 2885
- Cherchneff I., Le Teuff Y.H., Williams P.M., Tielens A.G.G.M., 2000, *A&A* 357, 572
- Cohen M., Barlow M.J. Liu X.-W., Jones A.F., 2002, *MNRAS* 332, 879
- Crowther P.A., 1997, *MNRAS* 290, L59
- Crowther P.A., 2003a, *Ap&SS* 285, 677
- Crowther P.A., 2003b, in proc IAU Symp 212, A Massive Star Odyssey, from Main Sequence to Supernova, (eds. K.A. van der Hucht, A. Herrer, C. Esteban), ASP: San Francisco, p.47
- Crowther P.A., Smith L.J., 1996, *A&A* 305, 531
- Crowther P.A., De Marco O., Barlow M.J., 1998, *MNRAS* 296, 367
- Crowther P.A., et al. 2002, *A&A* 392, 653
- De Marco O., Schmutz W., Crowther P.A. et al. 2000, *A&A* 358, 187
- De Marco O., Sandquist E.L., Maclow M-M., Herwig F., Taam, R.E.. 2003, in proc. The Eighth Texas-Mexico Conference on Astrophysics (eds. M. Reyes-Ruiz, E. Vazquez-Semadeni), *Rev Mex A&A Conf Ser* 18, 24
- Dessart L. et al. 2000 *MNRAS* 315, 407
- Eenens P.R.J., Williams P.M., 1994, *MMRAS*
- Gräfener, W.-R., Hamann, 2005, *A&A* 432, 633
- Grevesse N., Sauval A.J., 1998, *Space Sci Rev* 81, 161
- Hadfield L.J., Crowther P.A., Schild H., Schmutz W., 2005, *A&A* 439, 265

- Harries T.J., Minnier J.D., Symington N.H., Kurosawa R., 2004, MNRAS 350, 565
- Herwig F., Blöcker, T., Langer N., Driebe T., 1999, A&A 349, L5
- Herwig F., Lugaro M., Werner K., 2003, in proc IAU Symp 209, Planetary Nebulae: Their Evolution and Role in the Universe (eds. S. Kwok, M. Dopita, R. Sutherland), ASP: San Francisco, p.85
- Heydari-Malayeri M., Melnick J., van Drom E., 1990, A&A 236, L21
- Hillier D.J., 1991, A&A 247, 455
- Hillier D.J., Miller D.L., 1998, ApJ 496, 407
- Hirschi R., Meynet G., Maeder A., 2005, A&A in press (astro-ph/0507343)
- Hopewell E.C., Barlow M.J., Drew J.E. et al. 2005, MNRAS in press (astro-ph/0508187)
- Houck J.R., Roellig T.L., van Cleve J. et al. 2004, ApJS 154, 18
- Howarth I.D., Schmutz W., 1992, A&A 261, 503
- Iben Jr. I., Kaler J.B., Truran, J.W., Renzini A., 1983, ApJ 264, 605
- Jameson R.F., Longmore A.J., McLinn J.A., Woolf N.J., 1974, ApJ 190, 353
- Koesterke L., Hamann W.-R., 1995 A&A, 299, 503
- Koesterke L., Hamann W.-R., 1997 A&A 320, 91
- Leitherer C., Chapman J.M., Koribalski B., 1997, ApJ 481, 898
- Leuenhagen U., Hamann W.-R., Jeffery C.S., 1996, A&A 312, 167
- Li J., Harrington J.P., Borkowski K.J., 2002, AJ 123, 2676
- Liu X.-W., Barlow M.J., Cohen M. et al. 2001, MNRAS 323, 343
- Lodders K., 2003, ApJ 591, 1220
- Meynet G., Maeder A., 2003, A&A 404, 975
- Moffat A.F.J., 1991, A&A 244, L9
- Morris P.W., van der Hucht K.A., Crowther P.A., Hillier D.J., Dessart L., Williams P.M., Willis A.J., 2000, A&A 353, 624

- Nugis T., Lamers H.J.G.L.M., 2000, *A&A* 360, 227
- Prinja R.K., Barlow M.J., Howarth I.D., 1990, *ApJ* 361, 607
- Reiff E., Rauch T., Werner K., Kruk J.W., 2005, in *proc: White Dwarfs, ASP Conf Ser* (eds. D. Koester, S. Moehler), Vol 334, 225
- Runacres M., Owocki S., 2002 *A&A* 381, 1051
- Schaerer D., Maeder A., 1992, *A&A* 263, 129
- Siebenmorgen R., Zijlstra A.A., Krügel E., 1994, *MNRAS* 271, 449
- Smith J.D., Houck J.R., 2005, *ApJ* 622, 1044
- Smith L.F., Aller L.E., 1971, *ApJ* 164, 275
- Smith L.F., Hummer D.G., 1988, *MNRAS* 230, 511
- Smith L.F., Maeder A., 1991, *A&A* 241, 77
- Torres-Dodgen A., Massey P.M., 1988, *AJ* 96, 1076
- van der Hucht K.A., 2001, *New Astron.* 35, 145
- van der Hucht K.A. et al. 1996, *A&A* 315, L193
- Vink J.S., de Koter A., 2005, *A&A* in press (astro-ph/0507352)
- Waters L.B.F.M., Beintema D.A., Zijlstra A.A. et al. 1998, *A&A* 331, L61
- Williams P.M., van der Hucht K.A., 2000, *MNRAS* 314, 23
- Williams P.M., van der Hucht K.A., Thé P.S., 1987 *A&A* 182, 91
- Williams P.M., van der Hucht K.A., Rauw G., 2005, in *proc. Massive Stars and High-Energy Emission in OB Associations (JENAM 2005)*, astro-ph/0508157
- Willis A.J., Dessart L., Crowther P.A. et al. 1997, *MNRAS* 290, 371
- Willis A.J., Crowther P.A., Fullerton A.W. et al. 2004, *ApJS* 154, 651

Table 1: Stellar and wind properties of HD 164270 and BD+30 3639, including Lyman (Q_0) and HeI (Q_1) continuum ionizing photons.

Star	HD 164270	BD+30 3639
Sp Type	WC9	[WC9]
T_* (kK)	48	55
$T_{\tau=2/3}$ (kK)	41	48
$\log(L/L_\odot)$	4.90	3.78
R_*/R_\odot	4.1	0.85
$\dot{M}/\sqrt{f}(M_\odot\text{yr}^{-1})$	-4.50	-5.55
f	0.1	0.1
v_∞ (km/s)	1140	700
$\dot{M}v_\infty/(L/c)$	7	5
C/He	0.20	0.25
O/He	0.01	0.05
$M(M_\odot)$	6	0.6:
$\log Q_0$ (s^{-1})	48.57	47.50
$\log Q_1$ (s^{-1})	40.38	40.28
M_v (mag)	-4.6	-1.5

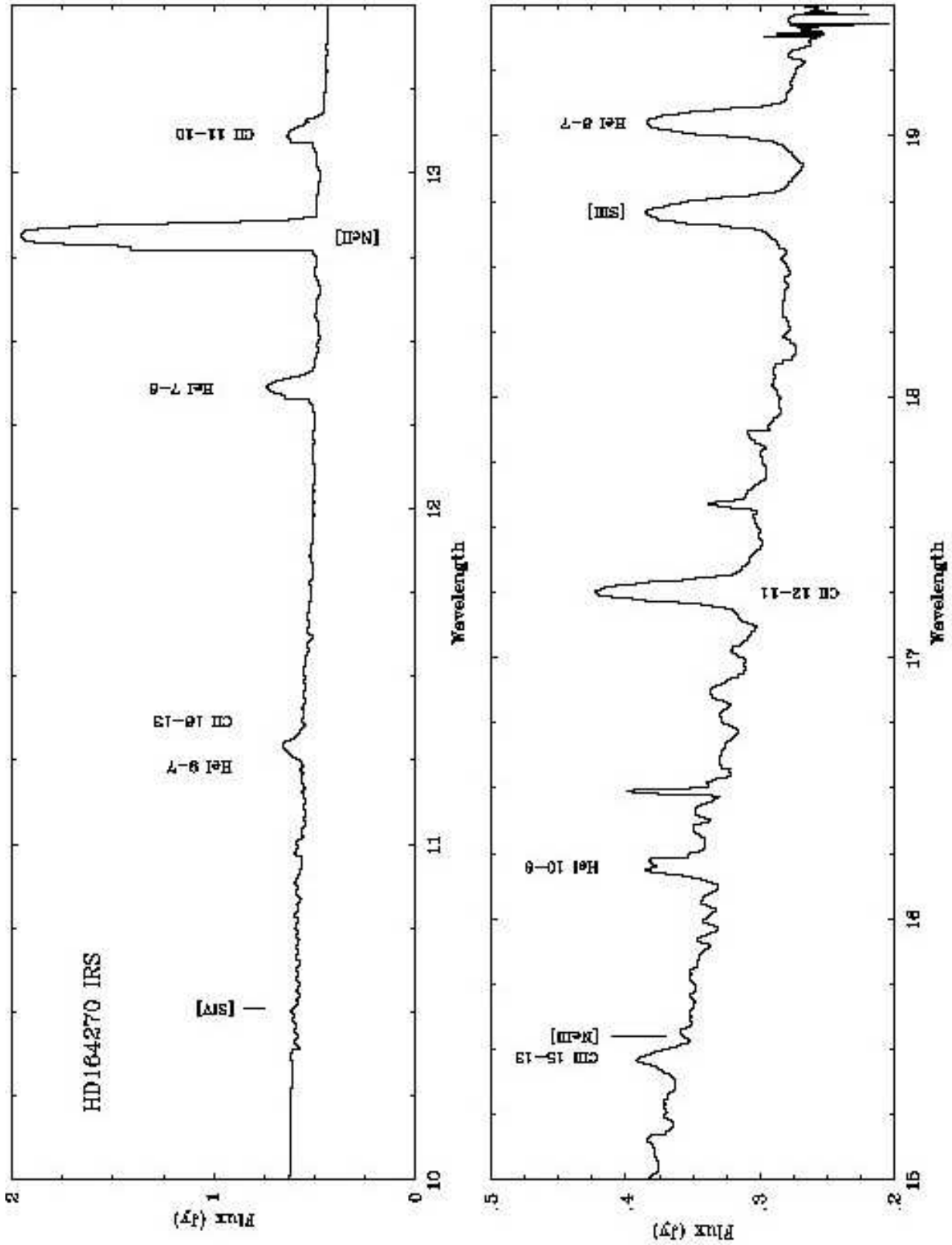


Fig. 1.— Selected regions of the IRS Short-High (SH) echelle spectrum ($R \approx 1000$) for HD 164270 (WC9).

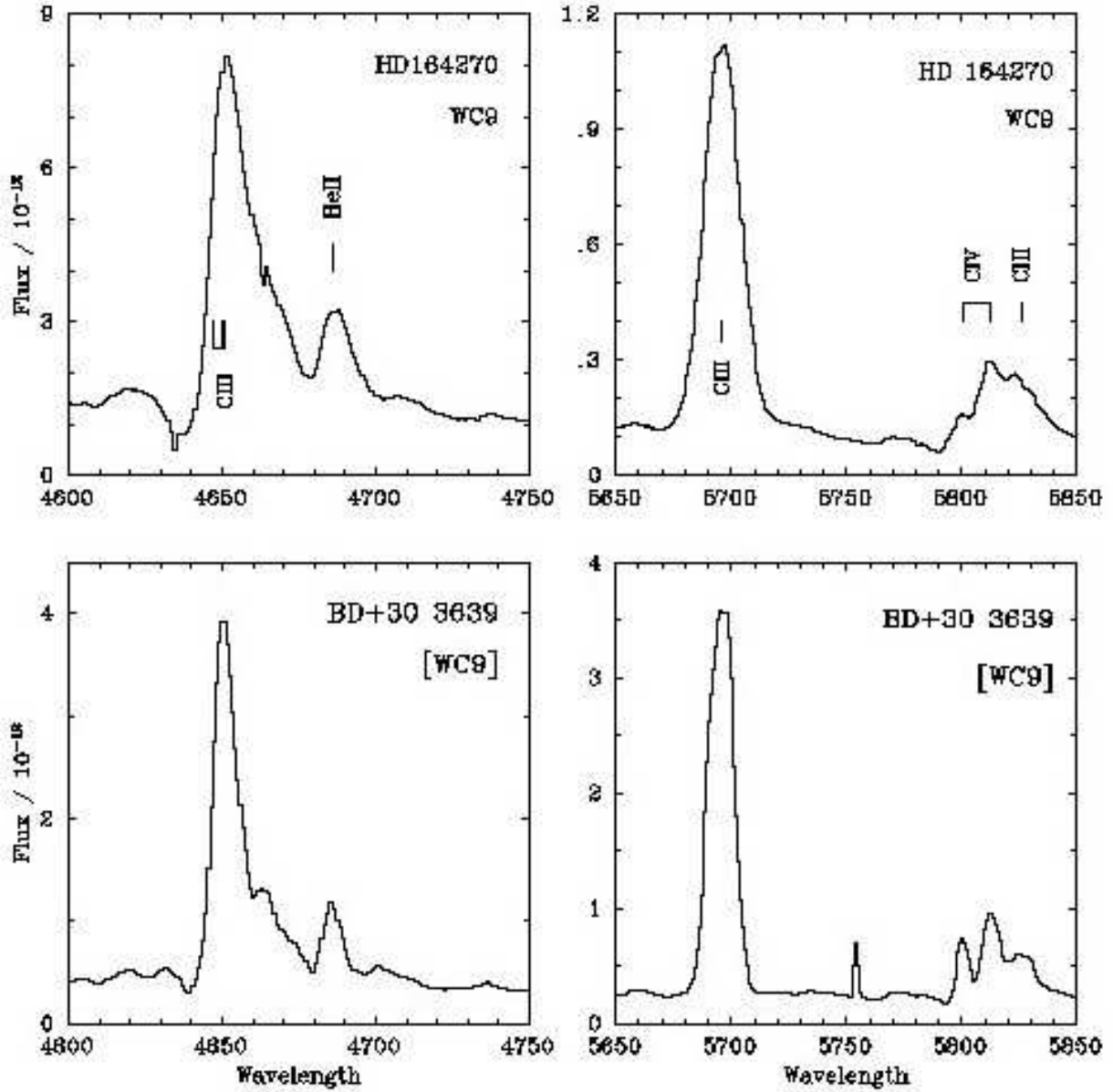


Fig. 2.— Spectroscopic comparison between HD 164270 (AAT/RGO, 1.7\AA resolution) and BD+30 3639 (WHT/ISIS, 3.5\AA resolution) in the vicinity of C III $\lambda 4650$ /He II $\lambda 4686$ and C III $\lambda 5696$ /C IV $\lambda 5801-12$, indicating a very similar appearance except for narrower lines in BD+30 3639, originating from a slower stellar wind.

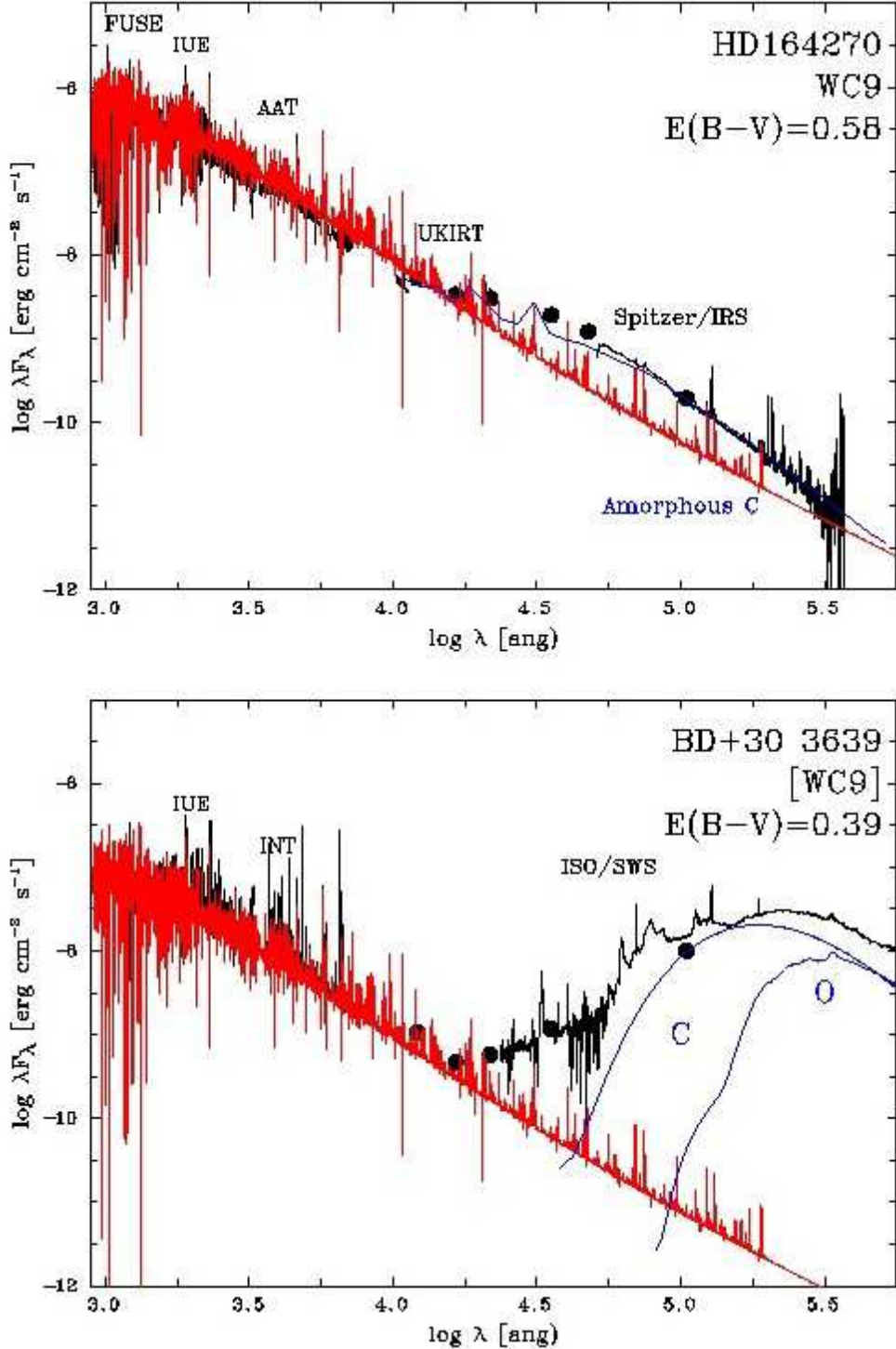


Fig. 3.— De-reddened spectral energy distributions (ergs⁻¹ cm⁻²) from 0.1-100 μ m for HD164270 (upper panel) and BD+30 3639 (lower panel), including ground-based JHKLMN photometry (solid circles), together with stellar continua from our analysis (red), dust distributions (green) from TORUS (Harries, priv. comm.) and MODUST (Waters et al. 1998). In both cases the stellar continuum dominates the flux distribution in the UV/optical, with dust contributing longward of 1 μ m. At 10 μ m the circumstellar dust in HD 164270 provides \sim 70% of the continuous flux, whilst the re-radiated dust from the PN of BD+30 3639

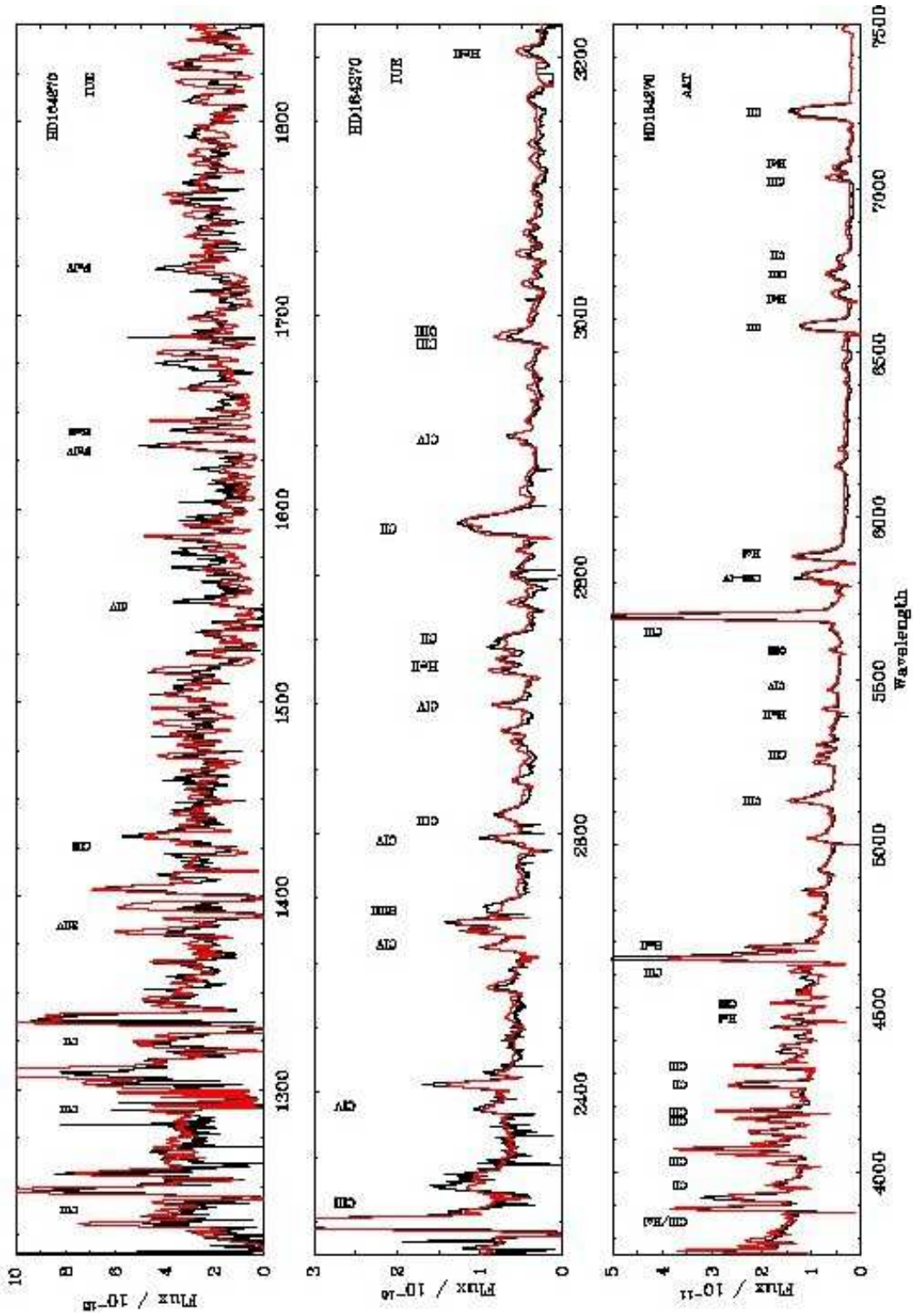


Fig. 4.— Spectroscopic fit (red) to de-reddened ($E(B-V)=0.58$ mag, $R=3.0$, $\log N(HI/cm^2)=21.0$), UV (IUE/HIRES, 0.1\AA resolution) and optical (AAT/RGO, 1.7\AA resolution) spectrophotometry of HD 164270 (WC9, black), including principal line identifications.

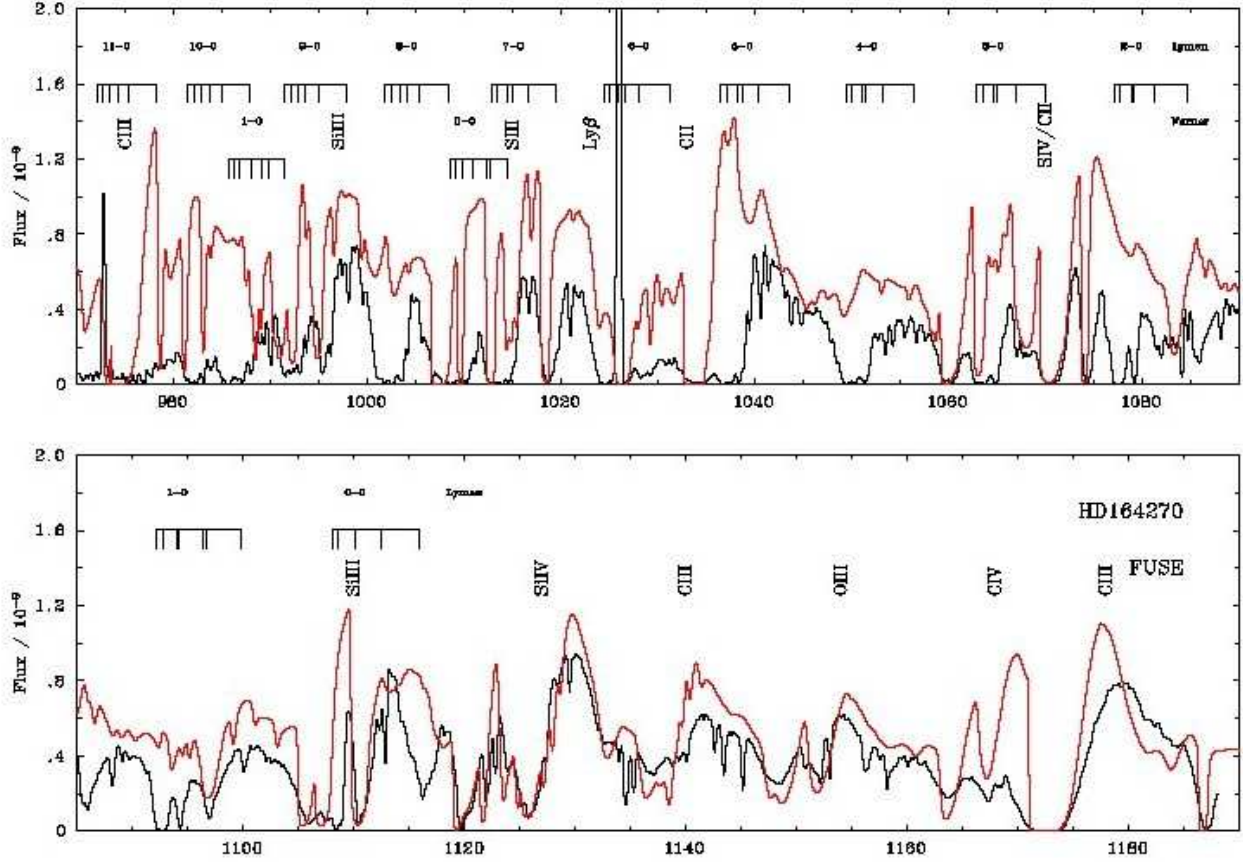


Fig. 5.— Comparison between de-reddened ($E(B-V)=0.58$ mag, $R=3.0$) *FUSE* far-UV spectrophotometry of HD 164270 (rebinned to 0.1\AA , Willis et al. 2004) and our synthetic spectrum (red), corrected for atomic hydrogen ($\log N(HI/\text{cm}^{-2})=21.0$), including principal line identifications. Leading components ($J=0-3$) of the Lyman and Werner molecular hydrogen bands are also indicated, which reveal that the stellar spectral range shortward of $\lambda 1120$ is increasingly contaminated by H_2 .

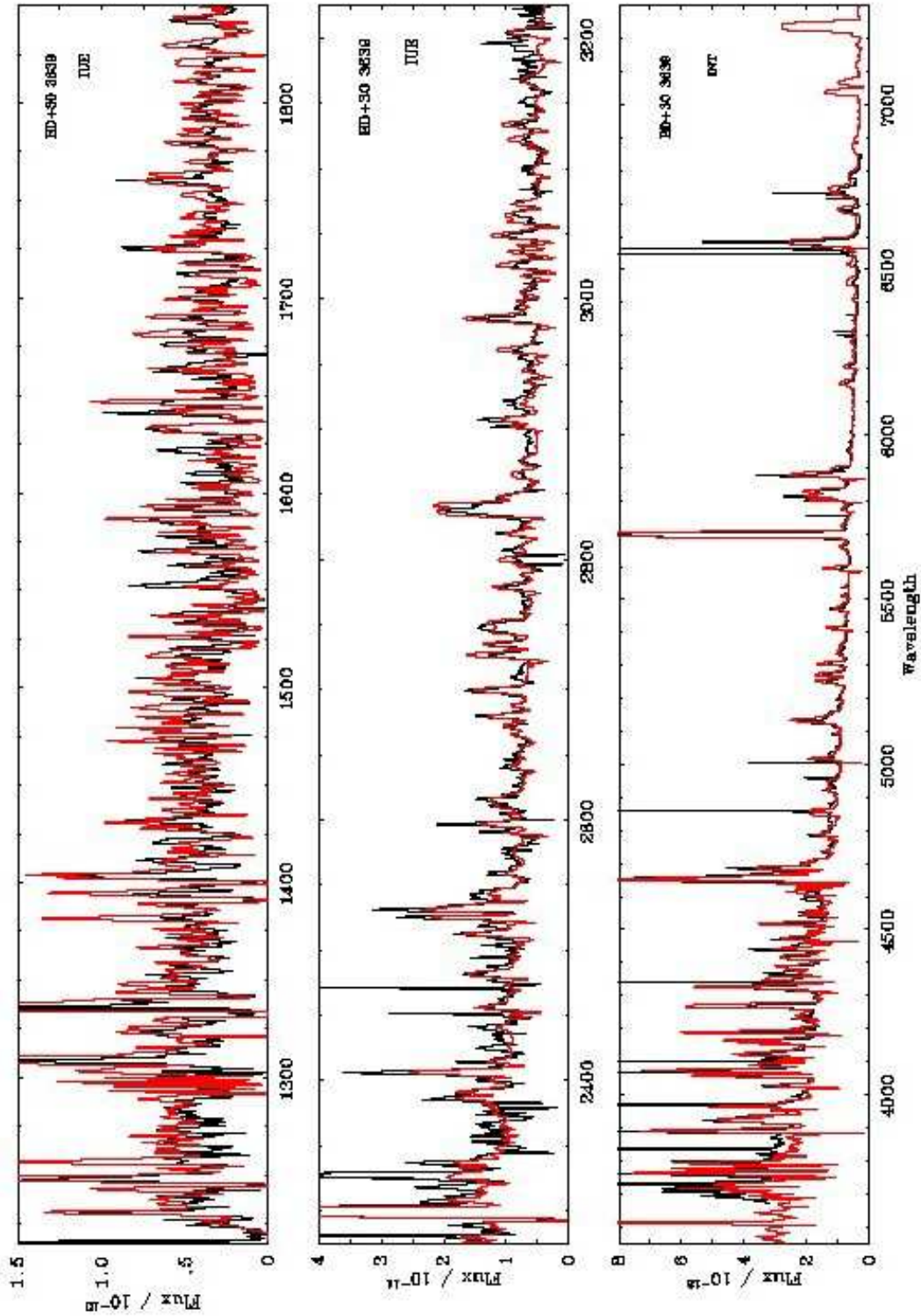


Fig. 6.— Spectroscopic fit (red) to de-reddened (E(B-V)=0.39, R=3.1, log N(HI/cm⁻²)=21.2), UV (IUE/HIRES, 0.1 Å resolution) and optical (WHT/ISIS, 3.5 Å resolution) spectrophotometry of BD+30 3639 ([WC9], black)

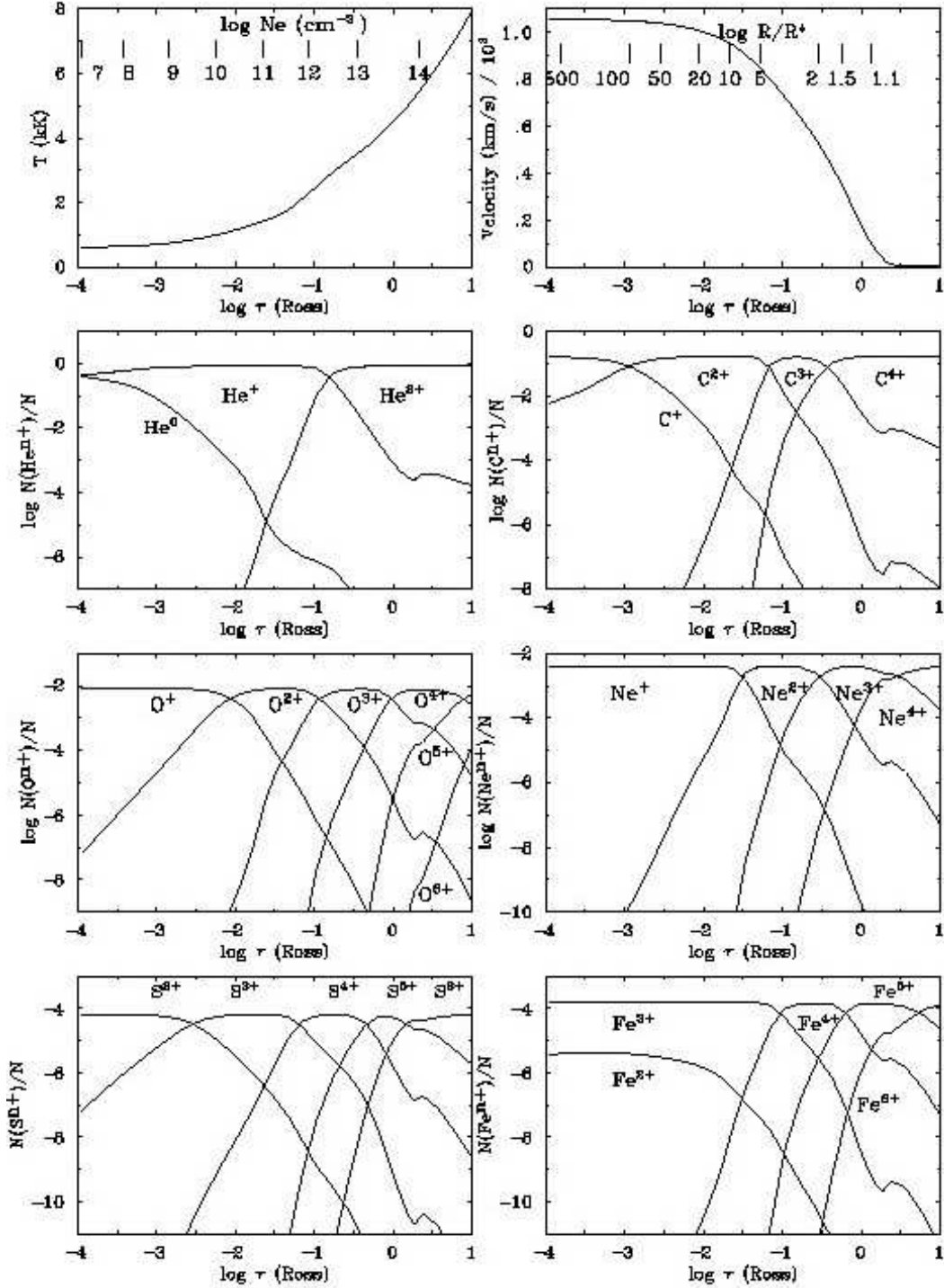


Fig. 7.— Predicted ionization balance of He, C, O, Ne, S and Fe for our HD 164270 model versus Rosseland optical depth, together with the electron temperature and density distribution and variation in wind velocity and radius with optical depth. This figure indicates that He is partially recombined in the outer wind of WC9 stars, affecting previous radio derived mass-loss rates (Leitherer et al. 1997; Cappa et al. 2004), plus supports dominant ionization stages of Ne^+ and S^{2+} for neon and sulfur, respectively, in agreement with *Spitzer* observations.

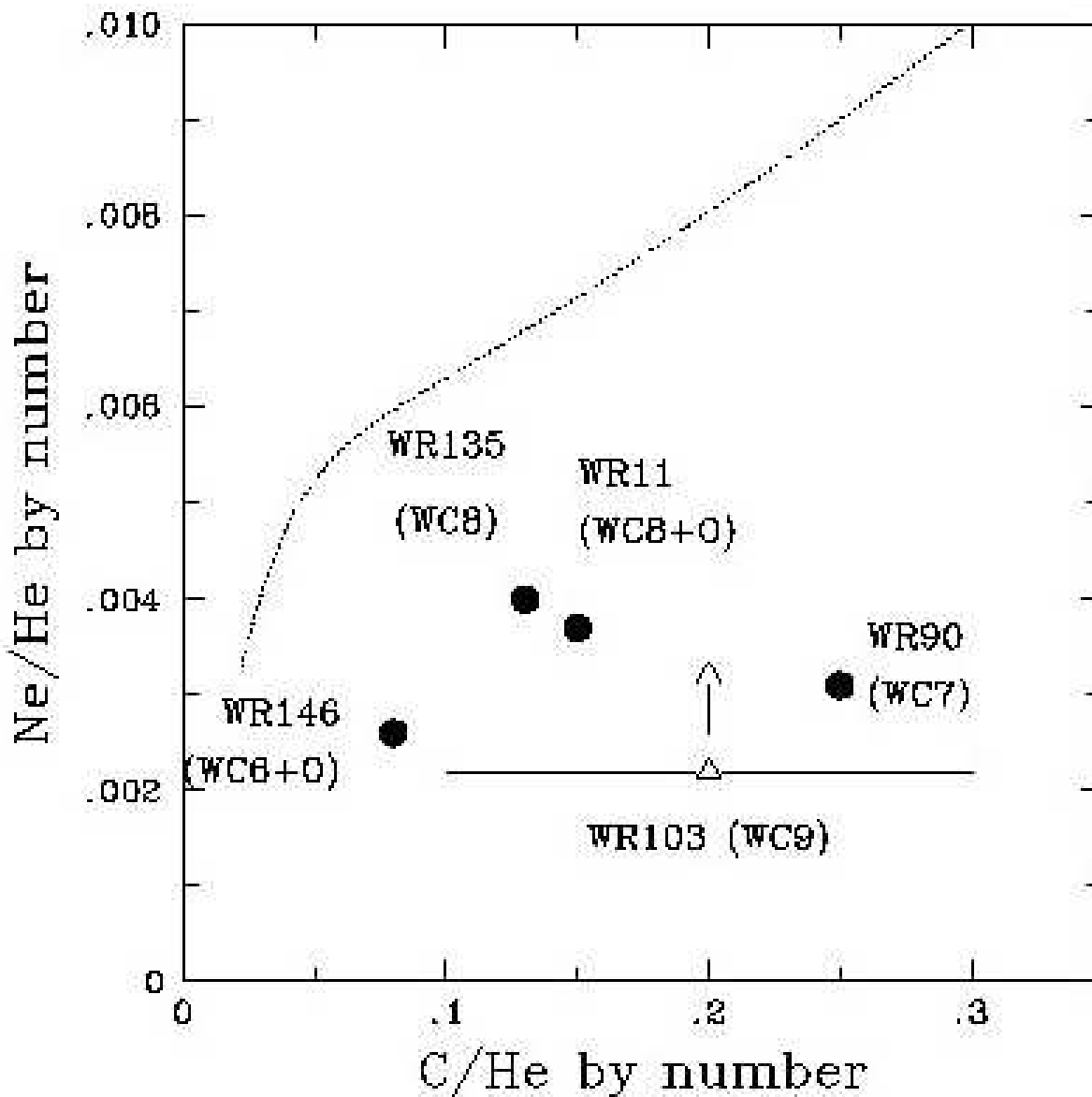


Fig. 8.— Comparison between carbon and neon abundances of HD 164270 (WC9, open triangle), by number, relative to other WC stars analysed in the same manner by Dessart et al. (2000, filled circles). We include predictions for the WC phase of star with initial mass $60M_{\odot}$ star at $Z=0.02$ rotating at 300 km/s from Meynet & Maeder (2003, dotted lines) which indicates that the measured neon abundances from analysis of mid-IR fine structure lines fall a factor of 2–3 times below predictions.

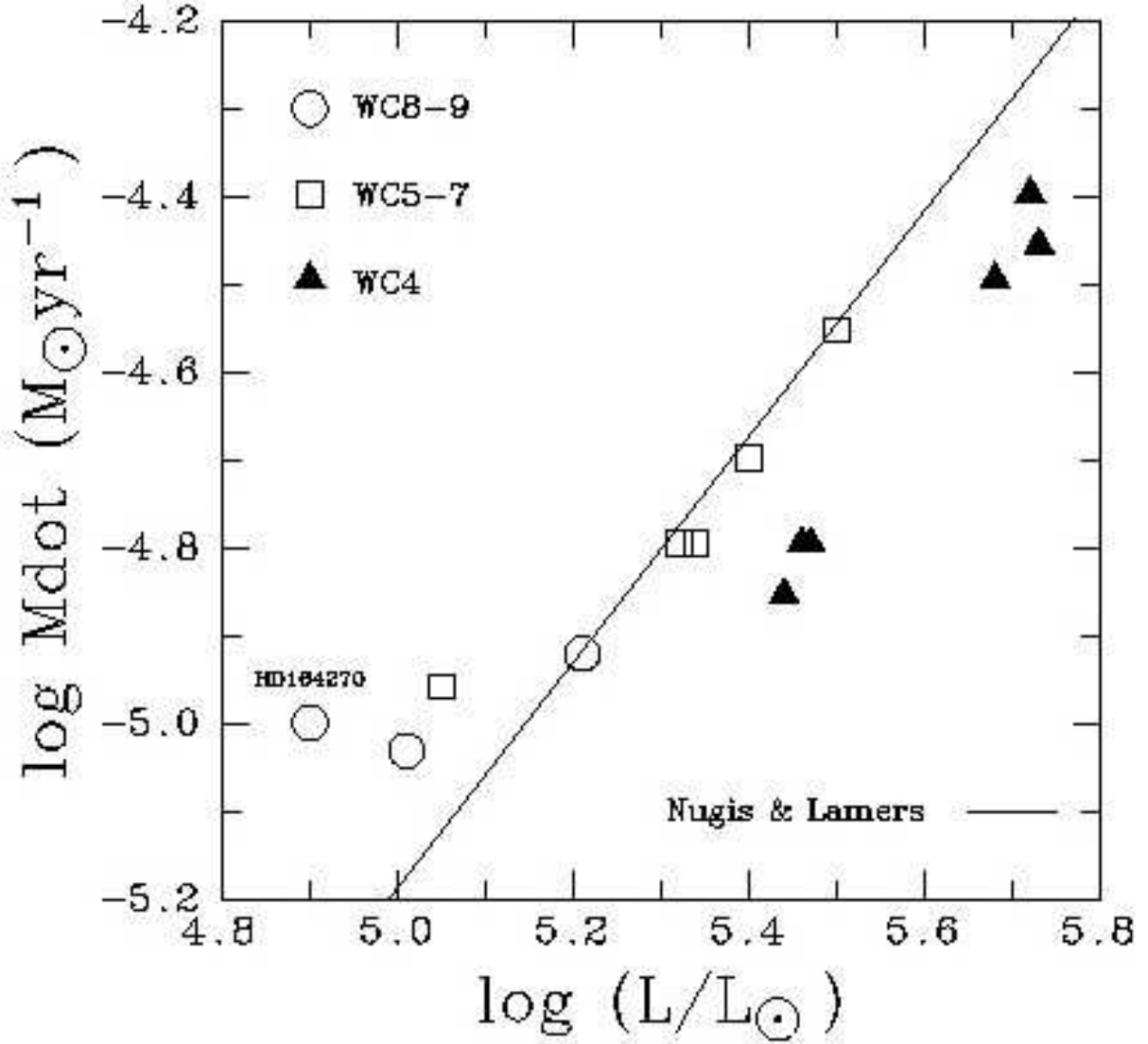


Fig. 9.— Comparison between mass-loss rates and luminosities of Galactic (open) and LMC (filled) WC stars from Crowther et al. (2002) and references therein, plus HD 164270 (WC9) newly studied here. As a guide, the generic Wolf-Rayet mass-loss luminosity relation from Nugis & Lamers (2000, their Eqn. 22) is presented for assumed abundances of C/He=0.25 and C/O=5 by number.